Relative docking and formation control via range and odometry measurements

Cao, Kun; Qiu, Zhirong; Xie, Lihua

2020

Cao, K., Qiu, Z., & Xie, L. (2020). Relative docking and formation control via range and odometry measurements. IEEE Transactions on Control of Network Systems, 7(2), 912-922. doi:10.1109/TCNS.2019.2951893

https://hdl.handle.net/10356/146206

https://doi.org/10.1109/TCNS.2019.2951893

Relative Docking and Formation Control via Range and Odometry Measurements

Kun Cao, Zhirong Qiu, and Lihua Xie, *Fellow, IEEE*

***Abstract*—This paper studies the problem of distance-based relative docking of a single robot and formation control of multi-robot systems. In particular, an integrated localization and navigation scheme is proposed for a robot to navigate itself to a desired relative position with respect to a fixed landmark at an unknown position, where only range and odometry measurements are used. By carefully embedding historical measurements into equilibrium conditions, we design an integrated estimation-control scheme to achieve the relative docking asymptotically. It is rigorously proved that the robot will converge to the desired docking position asymptotically provided that control gains are chosen to satisfy certain conditions. This scheme is further extended to multi-robot systems to consider an integrated relative localization and formation control problem. Unlike widely used spatial cooperation in existing literature, we propose to exploit both spatial and temporal cooperations for achieving formation control. It is proved that multi-robot formation can be achieved with zero error for directed acyclic graphs (DAG). Several simulation examples are provided to validate our theoretical results.**

***Index Terms*—Docking, range-only measurements, formation control, persistent excitation.**

I. Introduction

RECENT decade has witnessed a dramatic surge of robots which enjoy wide applications in civilian, industrial and military areas, such as cooperative search and exploration [1], environmental monitoring [2], aerial surveillance [3], accurate collaborative mapping [4], etc. Two fundamental problems, localization and navigation, have been investigated separately in robotics, control and signal processing communities, see [5]–[12] and the references therein.

As a subtopic of navigation, the docking problem has extensive applications in spacecraft, UAV precision landing and autonomous parking. When the relative position to a fixed landmark can be obtained, the docking problem can be readily solved by a naive proportional controller. Otherwise, it becomes quite challenging and requires an integrated localization and navigation scheme. In [13], the target pursuit problem with a fixed unknown landmark was addressed by adopting a diminishing persistent excitation to reconcile the localization and position tracking problems, where range and global position measurements are required. A similar idea is further applied in [14] to solve the station-keeping problem. However, the GPS signal may be not precise enough (meter accuracy in general) or even unavailable (e.g., indoor environments and urban canyons), and other positioning systems (e.g., UWB, VICON and WiFi) require extra infrastructures (e.g., anchors or cameras which are expensive), extensive labors and costs (e.g., deployment, calibration and maintenance). Recently, the authors in [15] introduced an integrated localization and navigation as a discrete-time counterpart of [13], where input saturation was explicitly considered and only self-displacement (odometry) and distance information are required. However, docking to a desired position with known relative position to a fixed unknown landmark, referred to as relative docking, is more general and practical since in many cases, for example in a search and rescue task, a beacon cannot be placed exactly at an unaccessible location such as roof top or a disaster site but at an accessible location with known relative position to the docking point. This problem is rather challenging since a single range measurement cannot indicate the proximity of the robot to the desired docking position.

On the other hand, formation control, navigation of multiple robots, can be regarded as a generalized relative docking problem for multiple robots. Existing research on formation control can be generally categorized into six classes according to the specification of the desired configuration: 1) position-based [16]; 2) displacement-based [17], [18]; 3) distance-based [19]; 4) bearing-based [20]; 5) angle-based [21]; and 6) ratio-of-distance-based [22]. Among the existing works and the references therein, almost all require relative position measurements except a few works, such as, range-only [23], [24] and bearing-only [20], [25] formation control. However, currently, no exteroceptive sensor can generate relative position measurements directly; they can only be obtained by data fusion of distance and bearing sensor measurements (e.g. LiDAR). As distance and bearing sensors sample at different times and frequencies, the accuracy of the fused relative position estimations may not be sufficient for highly accurate control. Therefore, it is highly preferable to design an integrated localization and formation control scheme to achieve desired configuration via bearing-only or range-only measurements. The authors in [26], [27] have proposed integrated schemes by using deterministic and probabilistic approaches for relative localization and formation control of multi-agent systems, respectively. However, notice that the localization and formation errors converge to zero only if the initial relative positions between agents are exactly known since the two objectives are conflicting, i.e., relative localization requires persistently excited measurements while formation control aims to keep

This work was supported by the ST Engineering-NTU Corporate Laboratory through the NRF Corporate Laboratory@University Scheme and Projects of Major International (Regional) Joint Research Program NSFC (Grant no. 61720106011). K. Cao, Z. Qiu and L. Xie (corresponding author) are with School of Electrical and Electronic Engineering, Nanyang Technological University, 50 Nanyang Avenue, Singapore 639798 (email: {kun001, qiuz0005}@e.ntu.edu.sg; elhxie@ntu.edu.sg).

agents relatively stationary. Furthermore, observe that most of the existing research on cooperative formation control focus on spatial cooperation, i.e., using inter-node measurements, while the other essential perspective, temporal cooperation which can be embodied as intra-node measurements, is not fully exploited. Some related ideas can be found in [12] and the references therein.

Motivated by the above observations, the first contribution of this work is to generalize the distance-based docking [15] to distance-based relative docking. This generalization is non-trivial since the distance measurement in the former can directly indicate whether the mission has been completed, i.e., zero distance measurement implies the exact docking, which is not the case for the latter. Inspired by the multi-lateration method in localization, we propose a novel motion controller which is triggered at several time instants (the number of triggering depends on the dimension and required accuracy) such that the distances measured at those time instants can signal the completion of a mission. Furthermore, the convergence of the system employing the proposed controller is proved via the discrete-time Lasalle's invariance principle [28] provided that the triggering positions satisfy some mild condition.

Secondly, we further extend this idea to the formation control problem and address the inherent conflict aroused in integrated localization and formation control [26] by applying the diminishing persistent excitation idea [13]–[15] or the adaptive radius assignment idea in [24]. The main idea is that each agent is performing a deliberate motion whose amplitude decreases with the formation error, which is delineated by the distance measurements at several triggering time instants. Compared to [24], [26], this work inherits the practicality of [15] by considering discrete-time formulation and input saturation; more importantly, the formation error is proved to converge to zero globally asymptotically under a proper parameter setting. Our proposed controllers require weaker graphical condition (directed acyclic graphs instead of being distance rigid) compared to [24] and take an explicit and continuous expression compared to [23], where only a descriptive stop-and-go strategy was given. Moreover, our proposed scheme can deal with high dimensional spaces while [23], [24], [26] can only achieve formation control in 2D space. A preliminary version of this work can be found in [29], where only the relative docking problem of a single robot is considered.

The remainder of this paper is structured as follows. Section II introduces some preliminaries and formulates the problems. Section III presents an integrated localization and navigation scheme for relative docking of a single robot. Section IV further extends this scheme to the integrated localization and formation control of multiple robots. Simulation results are given in Section V and the conclusion is finally drawn in Section VI.

II. Preliminaries

A. Notations

Throughout the paper, $\mathbb{R}, \mathbb{R}_+$ and $\mathbb{R}_{\geq 0}$ denote the sets of real numbers, positive real numbers and nonnegative real numbers, respectively. Let $\mathbb{Z}_+$ and $\mathbb{Z}_{\geq 0}$ represent the sets of positive integers and nonnegative integers, respectively. $\mathbb{R}^n$ and $\mathbb{R}^{m\times n}$ denote the sets of n-dimensional real vectors and $m \times n$ real matrices, respectively. $|c|$ is the absolute value of $c \in \mathbb{R}$. Let $\|x\|$ and $\|x\|_\infty$ denote the 2 norm and infinity norm for a vector $x \in \mathbb{R}^n$. Given a matrix $A \in \mathbb{R}^{n\times n}$, $A^\top, A^{-1}$ and $\|A\|$ are its transpose, inverse and induced 2 norm, respectively. Let $\mathrm{Diag}\{a_1, a_2, \cdots, a_n\}$ ($\mathrm{Diag}\{A_1, A_2, \cdots, A_n\}$) be the diagonal (block-diagonal) matrix with a_i (A_i) being its i-th diagonal entry (block). Let $I_n \in \mathbb{R}^{n\times n}$ be the identity matrix of dimension $n \times n$ and $\mathbf{0}_n$ the n-dimensional column vector with all entries of 0 or $n\times n$ zero matrix conformed to context. Let $\otimes$ denote the Kronecker product. Define $\mathcal{I}_n \coloneqq \{1, \cdots, n\}$ and $\mathrm{Card}(\mathcal{I})$ denotes the cardinality of a given set $\mathcal{I}$.

B. Graph Theory

A directed graph is defined as $\mathcal{G} = (\mathcal{V}, \mathcal{E})$, where $\mathcal{V}$ and $\mathcal{E} \subseteq \mathcal{V} \times \mathcal{V}$ denote the node set and edge set, respectively. Agent j is regarded as a neighbor of agent i if $(j, i) \in \mathcal{E}$, which means agent i can access the information of agent j. The neighbor set of agent i is denoted as $\mathcal{N}_i = \{j : (j, i) \in \mathcal{E}, j \in \mathcal{V}, j \neq i\}$. A walk is an ordered sequence of nodes such that any two consecutive nodes in the sequence correspond to an edge of the digraph. A path is a walk with no repeated vertices, i.e., a sequence of vertices $v_1, \cdots, v_k$ with $(v_i, v_{i+1}) \in \mathcal{E}, \forall i \in \mathcal{I}_{k-1}$ is called a path from node v_1 to node v_k. $|(v_1, v_k)|$ denotes the length of the path from v_1 to v_k. A cycle is defined as a walk which starts and ends at the same node with all other nodes on the walk being distinct. A digraph without cycles is a directed acyclic graph (DAG). The adjacency matrix $\mathcal{A} = (a_{ij}) \in \mathbb{R}^{N\times N}$ of $\mathcal{G}$ is defined as follows: $a_{ij} > 0$ if $(j, i) \in \mathcal{E}$ and $a_{ij} = 0$ otherwise, $i, j \in \mathcal{V}$. In addition, we assume that $\mathcal{G}$ does not include self loops, i.e., $a_{ii} = 0, \forall i \in \mathcal{V}$. The degree matrix of graph $\mathcal{G}$ is defined as $\mathcal{D} = \mathrm{Diag}\{\deg_1, \deg_2, \cdots, \deg_N\} \in \mathbb{R}^{N\times N}$, where $\deg_i = \sum_{j=1}^N a_{ij}$. The Laplacian matrix of $\mathcal{G}$ is then defined as $\mathcal{L} = \mathcal{D} - \mathcal{A} \in \mathbb{R}^{N\times N}$. A leader node labeled 0 is added to the graph $\mathcal{G}$ with $a_{i0} > 0$ if agent i can access agent 0's information and $a_{i0} = 0$ otherwise. Denote the resultant graph by $\overline{\mathcal{G}} = (\overline{\mathcal{V}}, \overline{\mathcal{E}})$ with $\overline{\mathcal{N}_i} = \{j : (j, i) \in \overline{\mathcal{E}}, j \in \overline{\mathcal{V}}, j \neq i\}$ and let $a_{0i} = 0$ for all $i \in \mathcal{V}$ and $\mathcal{L}_0 = \mathcal{L} + \mathrm{Diag}\{a_{10}, a_{20}, \cdots, a_{N0}\}$.

C. Problem Statement

1) Single robot relative docking: Consider a single robot whose motion is modeled by single-integrator with bounded input:

$$p_{k+1} = p_k + T\overline{u}_k, \|\overline{u}_k\|_\infty \leq U, \tag{1}$$

where $p_k \in \mathbb{R}^n$, T and U denote the position of the robot at time instant k, the sampling period and maximal velocity, respectively. Given a fixed landmark at an unknown position $p^* \in \mathbb{R}^n$ ($n = 2, 3$), we aim to dock a robot to a position relative to p^* by $x^* \in \mathbb{R}^n$, i.e.,

$$\lim_{k\to\infty} p_k = p^* + x^*, \tag{2}$$

based on range measurements $d_k = \|p_k - p^*\|$ and odometry measurements $\phi_k = T\overline{u}_k$. The problem can be formally defined as follows:

Problem II.1. *Given the relative position x^*, design a controller $\overline{u}_k$ based on the distance measurements $d_k = \|p_k - p^*\|$ and self displacements, such that $p_k \to p^* + x^*$ as $k \to +\infty$.*

2) Multi-robot formation control: Consider a team of N robots with single-integrator dynamic model:

$$p_{k+1}^i = p_k^i + T\overline{u}_k^i, \|\overline{u}_k^i\|_\infty \leq U, i \in \mathcal{V}, \tag{3}$$

where $p_k^i \in \mathbb{R}^n$ and $\overline{u}_k^i \in \mathbb{R}^n$ denote the position and control input of robot i, respectively. Given a fixed landmark at an unknown position and assume that part of robots have range measurements to the landmark, we aim to cooperatively navigate the team of robots to the prescribed relative position $x_i^*, i \in \mathcal{V}$, i.e.,

$$\lim_{k\to\infty} p_k^i = p^* + x_i^*, i \in \mathcal{V}, \tag{4}$$

based on range measurements $d_k^{ij} = \|p_k^i - p_k^j\|$, odometry measurements $\phi_k^i = T\overline{u}_k^i$ and local communications. In the above, the underlying graph for measurements and communications is described by $\overline{\mathcal{G}}$ (defined in Sec. II-B) with the landmark being the leader node labeled "0". We formally state the problem as follows:

Problem II.2. *Given relative positions x_i^* to p^*, $i \in \mathcal{V}$, design a distributed controller $\overline{u}_k^i$ for each robot i, where only the distance measurements $d_k^{ij} = \|p_k^i - p_k^j\|$, $j \in \overline{\mathcal{N}}_i$, self displacements and local communications are available, such that $p_k^i \to p^* + x_i^*$, $i \in \mathcal{V}$, as $k \to +\infty$.*

The following assumption is presented first.

Assumption II.3. *$\overline{\mathcal{G}}$ satisfies the following conditions:*

1) *$\overline{\mathcal{G}}$ is a directed acyclic graph with the landmark "0" being the root; and*
2) *the inequality*

$$\sum_{j\in\overline{\mathcal{N}}_i} a_{ij} < 1, \tag{5}$$

holds for all $i \in \mathcal{V}$.

Remark II.4. *Assumption II.3 is mild and can be easily fulfilled. DAGs are a general class of graphs, which have been widely used in formation control with leader-follower architectures [30], [31]. Given a general topology, we can select a DAG as in [32]. (5) can be easily satisfied by choosing a_{ij} according to $\mathrm{Card}(\overline{\mathcal{N}}_i)$ [33].*

$\overline{\mathcal{G}}$ has a hierarchical structure and can be partitioned into $L+1$ layers according to the longest path from 0 to i, i.e., $\overline{\mathcal{V}} = \cup_{l=0}^{L}\mathcal{V}_l$ with $\mathcal{V}_0 = \{0\}$ and $\mathcal{V}_l = \{i \in \mathcal{V} : \max|(0,i)| = l\}$, $l \in \mathcal{I}_L$. Additionally, for each agent $i \in \mathcal{V}_l$, one has $j \in \mathcal{U}_{l-1} := \cup_{m=0}^{l-1}\mathcal{V}_m$ for its neighboring agent $j \in \overline{\mathcal{N}}_i$. Therefore, $\overline{\mathcal{G}}$ can be considered as a concatenation of L layers of leader-follower structures with $\mathcal{U}_{l-1}$ and $\mathcal{V}_l$ ($l \in \mathcal{I}_L$) being the leader(s) and the follower(s) in each structure, respectively.

Remark II.5. *It can be found that Problem II.1 is the simplest case of Problem II.2 when $L = 1$, $\mathcal{V}_1 = \{1\}$ and no local communications are involved. We will first address the former in the next section as a stepping stone to handle the latter, which is more complicated. Nevertheless, these two problems may have different potential applications: the former can be applied to many cases in adversarial environments (no GPS signal is available and anchor cannot be placed exactly at the target position), ranging from airdrops for disaster relief or water tanks for forest fire-fighting, to navigation of various unmanned vehicles [34]; the latter can be applied to environmental monitoring with large-scale swarms subject to limited budgets since it has weaker requirements on sensor measurements.*

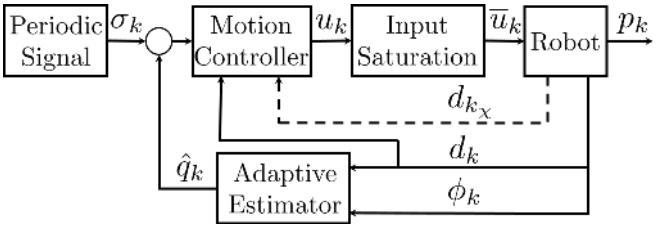

Fig. 1: An illustration of the robot's control diagram for relative docking. d_k and ϕ_k are from range sensor and odometer, respectively. d_{k_χ} is range measurement at some triggering time instant, which will be elaborated in subsection III-A.

III. Integrated localization and navigation for relative docking

In this section, we present an integrated localization and navigation scheme to tackle Problem II.1. Specifically, as shown in Fig. 1, we design an adaptive estimator for estimating the desired docking position with distance measurements from range sensor and self displacements from odometer. Then this estimate is used in the proposed motion controller for navigating the robot to the desired docking position.

A. Adaptive Estimator

Let $q_k = p_k - (p^* + x^*)$ and $\hat{q}_k$ be the estimate of q_k. It follows from (1) that

$$q_{k+1} = q_k + \phi_k. \tag{6}$$

On the other hand, notice that

$$\begin{aligned} d_{k+1}^2 - d_k^2 &= \|p_{k+1} - p^*\|^2 - \|p_k - p^*\|^2 \\ &= \|q_{k+1} + x^*\|^2 - \|q_k + x^*\|^2 \\ &= \|\phi_k\|^2 + 2\phi_k^\top(q_k + x^*), \end{aligned} \tag{7}$$

from which the following adaptive updating law can be designed:

$$\hat{q}_{k+1} = \hat{q}_k + \phi_k + \Gamma\phi_k\epsilon_{k+1}, \tag{8}$$

where $\epsilon_{k+1} = \frac{1}{2}(d_{k+1}^2 - d_k^2 - \|\phi_k\|^2) - \phi_k^\top(\hat{q}_k + x^*) = \phi_k^\top(q_k + x^*) - \phi_k^\top(\hat{q}_k + x^*)$, $\Gamma \in \mathbb{R}^{n\times n}$ and $0 < \Gamma < \gamma I_n$.

B. Motion Controller

We first introduce a function f and a periodic signal σ_k that will be used in our proposed motion controller.

$f : \mathbb{R}_{\geq 0} \to \mathbb{R}_{\geq 0}$ is a function satisfying the following assumption:

Assumption III.1. *$f(0) = 0$, and $0 < f(x) \leq x$, $\forall x > 0$.*

σ_k is an external signal generated from an autonomous system [15]:

$$\begin{aligned} \rho_{k+1} &= \Pi(\rho_k), \\ \sigma_k &= \Sigma(\rho_k), k \in \mathbb{Z}_{\geq 0}, \end{aligned} \tag{9}$$

where $\Pi(\cdot)$ and $\Sigma(\cdot)$ are two continuous mappings to be chosen. The autonomous system (9) is introduced for reconciling two conflicting objectives: adaptive estimation of docking position and navigation. In other words, the adaptive estimator (8) requires excited motion for convergence, while the motion controller tends to navigate the robot to a fixed position. Thus, the autonomous system needs to persistently perturb the robot's motion until reaching the docking point, and the magnitude of the perturbation should decrease as the robot approaches the docking point. Specifically, σ_k is required to be constructed such that the following assumption holds:

Assumption III.2. *[15] 1) ρ_k is bounded, $\forall k \in \mathbb{Z}_{\geq 0}$, and $\sup_{k\in\mathbb{Z}_{\geq 0}} \|\sigma_k\| \leq 1$; and*
2) there exists some constant $\tau_0 \in \mathbb{Z}_+$ such that $\sigma_{k+\tau_0} = -\sigma_k$, $\forall k \in \mathbb{Z}_{\geq 0}$ and $\mathrm{Span}\{\sigma_0, \cdots, \sigma_{\tau_0-1}\} = \mathbb{R}^n$.

Remark III.3. 1) *Assumption III.1 can be easily satisfied by choosing $f(x) = x$ and other choices can be found in [13] and references therein;*

2) *For $n = 2$, Assumption III.2 can be fulfilled by choosing $\rho_0 \in \mathbb{R}^2$ with $\|\rho_0\| = 1$, $\Sigma = I_2$ and $\Pi = \begin{bmatrix} \cos(2\pi/a) & -\sin(2\pi/a) \\ \sin(2\pi/a) & \cos(2\pi/a) \end{bmatrix}$ with $a \geq 4$ being an even integer. For $n = 3$, ρ_0 and Π remain the same as in the case of $n = 2$ while $\Sigma([\rho_{0,1} \ \rho_{0,2}]^\top) = [b_1\rho_{0,1} \ b_1\rho_{0,2} \ b_2(4\rho_{0,1}^3 - 3\rho_{0,1})]^\top/(b_1^2 + b_2^2)$, $\rho_0 = [\rho_{0,1} \ \rho_{0,2}]^\top$ [15].*

With a careful design of f and σ_k, a bounded motion controller for the robot is proposed as follows:

$$\overline{u}_k = \mathrm{proj}_U\, u_k, u_k = -\beta\hat{q}_k + Cf(\xi_k)\sigma_k, \tag{10}$$

where $\mathrm{proj}_U(\cdot)$ is a projection operator defined by

$$\mathrm{proj}_U\, u_k = \frac{U}{\max(U, \|u_k\|)} u_k \coloneqq s_k u_k \tag{11}$$

and

$$\begin{aligned} \xi_k &= \max(\zeta_k, |d_k - \|x^*\||), \\ \zeta_k &= \max_{\chi\in\{1,\cdots,\overline{n}\}} (|\|x^* - \sum_{t=k_\chi}^{k} \phi_t\| - d_{k_\chi}|), \overline{n} \geq n, \end{aligned} \tag{12}$$

with k_χ being the time step triggering the running sum term $\sum_{t=k_\chi}^{k} \phi_t$ and d_{k_χ} being the distance measurement at the same time with respect to the landmark. In comparison with [15], ζ_k is carefully designed by using accumulated odometry measurements $\sum_{t=k_\chi}^{k} \phi_t = p_k - p_{k_\chi}$ and past distance measurement d_{k_χ}, where p_{k_χ} should be chosen properly and its condition will be given later. In real implementation, the running sum term will accumulate error with respect to time. To alleviate this effect, we can apply the controller (8) in [15] to quickly approach $\mathcal{S}^{n-1}(p^*, \|x^*\|)$ first and choose p_{k_χ} near $\mathcal{S}^{n-1}(p^*, \|x^*\|)$. Furthermore, the running sum can be replaced by subtracting the buffered fused estimates (by onboard camera and IMU) of position at the triggering time instants from the current fused estimates, which is obtained from the off-the-shelf flight controller.

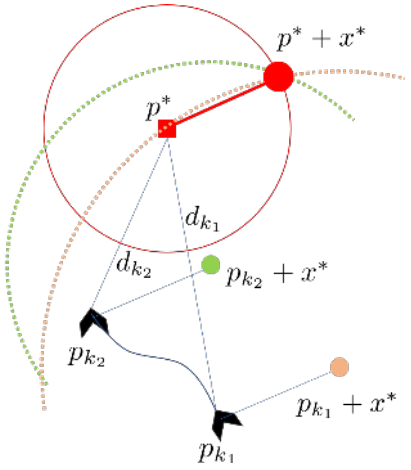

Fig. 2: An illustration of triggering in 2-D.

We first provide some insight of our controller design. Suppose $\overline{n} = n = 2$, then the three constraints in $\xi_k = 0$ form three circles which can be expressed by $d_k = \|p_k - p^*\| = \|x^*\|$ and $d_{k_\chi} = \|p_k - (p_{k_\chi} + x^*)\|$, $\chi = 1, 2$, see Fig. 2. The intersection point corresponds to $p_k = p^* + x^*$. This idea is closely related to multi-lateration approaches, if we regard p^*, $p_{k_1} + x^*$ and $p_{k_2} + x^*$ as the positions of three transmitters and $p^* + x^*$ as that of a receiver. However, whether $p^* + x^*$ can be uniquely determined depends on the choice of p_{k_χ}, and we need the following assumption.

Assumption III.4. *The coordinates of $\overline{n}$ triggering points $\{p_{k_\chi}\}_{\chi=1}^{\overline{n}}$ satisfy $\mathrm{Rank}([\cdots, p_{k_\chi} - p^* + x^*, \cdots]) = n$, $\chi = 1, \cdots, \overline{n}$.*

Remark III.5. *Compared with docking problem [15], where a single range measurement implies exact docking, i.e., $d_k = 0 \Rightarrow p_k = p^*$, it is not the case for relative docking, i.e., $d_k = \|x^*\| \not\Rightarrow p_k = p^* + x^*$. Therefore, relative docking is more challenging and require more measurements ((12)) which satisfy certain condition (Assumption III.4).*

Remark III.6. *Assumption III.4 can be easily fulfilled, e.g., the agent can move $n - 1$ random step(s) and record the displacement(s) and distance measurement(s) at the beginning. This idea shares some similarity with the station keeping problem [14]; actually, our method can be considered as putting $\overline{n}$ artificial landmarks along the motion trajectory in addition to the fixed landmark at p^*. However, [14] requires GPS which may not be available for many environments. Furthermore, we consider the discrete-time controller design, which can be implemented directly. The strategy of a mobile sensor triplet unit (MSTU) in [35] can be regarded as a special case of (12), where we can replace the term $\sum_{t=k_\chi}^{k} \phi_t$ and d_{k_χ} with a known spacing between two receivers and the distance measurement of one of them, respectively.*

C. Stability Analysis

In this section, we shall provide the stability analysis of the closed-loop system in the integrated scheme. To this end, the following result should be presented firstly.

Lemma III.7. *If Assumption III.4 holds, then* $\xi_k = 0$ *implies* $p_k = p^* + x^*$.

Proof. Let $q^* = p^* + x^*$ and $q_\chi = p_{k_\chi} - p^*$. $\xi_k = 0$ implies $\|p_k - q^* + x^*\| = \|x^*\|$ and $\|p_k - q^* - q_\chi\| = \|q_\chi\|$. Taking square on both sides, one has

$$\begin{aligned} \|p_k - q^*\|^2 &= -2(p_k - q^*)^\top x^*, \\ \|p_k - q^*\|^2 &= 2(p_k - q^*)^\top q_\chi, \chi = 1, \cdots, \overline{n} \end{aligned} \tag{13}$$

Subtracting them, we have $(p_k - q^*)^\top (q_\chi + x^*) = 0$ for all $\chi = 1, \cdots, \overline{n}$, and $p_k = q^*$ if $\mathrm{Rank}([\cdots, q_\chi + x^*, \cdots]) = n$. ∎

Remark III.8. *Assumption III.4 is sufficient but not necessary since* $\xi_k = 0 \Rightarrow p_k = q^*$ *still holds if* q^* *lies on the surface of the simplex formed by at most* $n+1$ *elements in* $\{p^*\} \cup \{p_{k_\chi} + x^*\}_{\chi=1}^{\overline{n}}$. *For example, if* $x^* = 0$, *we can simply set* $\zeta_k = 0$, *and recover the controller for the docking problem studied in [15].*

In the following two propositions, we establish the conditions of control gains for guaranteeing the boundedness of the closed-loop system.

Proposition III.9. *Under the adaptive estimator* (8), $\tilde{q}_k := \hat{q}_k - q_k \in \ell_\infty$ *and* $\epsilon_k \in \ell_\infty \cap \ell_2$ *if*

$$\gamma (TU)^2 < 2. \tag{14}$$

Proof. See Appendix A. ∎

Proposition III.10. *Under the motion controller* (10), *there exists a constant* M *such that* $\limsup_{k\to\infty} \|q_k\| \le M$ *if condition* (14) *holds and*

$$C < \beta < 1/T. \tag{15}$$

Proof. See Appendix B. ∎

Now, we are ready to establish the convergence result of the relative docking.

Theorem III.11. *Under Assumptions III.1, III.2 and III.4, Problem II.1 with dynamic model* (1) *can be solved by adopting adaptive estimator* (8) *and motion controller* (10) *with gains satisfying* (14) *and* (15).

Proof. The overall system under controller (6), (8), (10) and (9) can be written as

$$\begin{aligned} q_{k+1} &= q_k + \phi_k, \\ \tilde{q}_{k+1} &= (I - \gamma \phi_k \phi_k^\top)\tilde{q}_k, \\ \rho_{k+1} &= \Pi(\rho_k). \end{aligned} \tag{16}$$

By the boundedness result of Propositions III.9 and III.10, as well as Assumption III.2, we can invoke Lasalle's invariance principle [28] to show that all trajectories will converge to the largest invariant set $\mathcal{M}$ included in $\{[q_k^\top, \tilde{q}_k^\top, \rho_k^\top]^\top \in \mathbb{R}^{3n} \mid \Delta V_k = 0\}$, where V is the Lyapunov function defined in the proof of Proposition III.9. It suffices to show that $q_k \equiv 0$ holds for any trajectory $\{[q_k^\top, \tilde{q}_k^\top, \rho_k^\top]^\top\}_{k\in\mathbb{Z}_{\ge 0}}$ in $\mathcal{M}$.

By (30), we have $\Delta V_k \equiv 0$ iff $\epsilon_{k+1} = -\phi_k^\top \tilde{q}_k \equiv 0$, which also follows from (29) that $\tilde{q}_k \equiv \tilde{q}^{ss}$ for some constant $\tilde{q}^{ss}$. It suffices to show that $\phi_k^\top \tilde{q}_k \equiv 0$ is equivalent to $q^{ss} = 0$. Consider the following three cases:

1) $\phi_k \not\equiv 0$ and $\tilde{q}^{ss} \neq 0$. In this case, since
$$0 \equiv \phi_k^\top \tilde{q}_k = (q_{k+1} - q_k)^\top \tilde{q}^{ss} = (\hat{q}_{k+1} - \hat{q}_k)^\top \tilde{q}^{ss},$$
one has $\hat{q}_k^\top \tilde{q}^{ss} \equiv c^\dagger$ for some constant $c^\dagger \in \mathbb{R}$. Moreover, $0 \equiv \phi_k^\top \tilde{q}^{ss}$ also implies that $0 \equiv \phi_k^\top \tilde{q}^{ss} = [-\beta \hat{q}_k + Cf(\xi_k)\sigma_k]^\top \tilde{q}^{ss}$, or equivalently $\beta c^\dagger \equiv \beta \hat{q}_k^\top \tilde{q}^{ss} = Cf(\xi_k)\sigma_k^\top \tilde{q}^{ss}$. Specifically, we have $f(\xi_k)\sigma_k^\top \tilde{q}^{ss} = f(\xi_{k+\tau_0})\sigma_{k+\tau_0}^\top \tilde{q}^{ss}$. Next we establish $f(\xi_k) > 0$ by contradiction. Suppose $f(\xi_k) = 0$, then $\xi_k = \max(\zeta_k, |d_k - \|x^*\||)$, or equivalently $d_k = \|x^*\|$ and $\|x^* - \sum_{t=k_\chi}^{k} \phi_t\| = d_{k_\chi}$ for $\chi \in \{1, \cdots, \overline{n}\}$, which implies $p_k = p^* + x^*$ by Assumption III.4 and Lemma III.7. Then it follows from $u_k = -\beta \hat{q}_k = -\beta \tilde{q}^{ss}$ that $\phi_k^\top \tilde{q}^{ss} = Ts_k u_k^\top \tilde{q}^{ss} = -\beta T s_k \|\tilde{q}^{ss}\|^2 \neq 0$, a contradiction. Therefore, $f(\xi_k) > 0$, $\forall k \in \mathbb{Z}_{\ge 0}$. On the other hand, by $\sigma_{k+\tau_0} = -\sigma_k$, we have
$$[f(\xi_k) + f(\xi_{k+\tau_0})]\sigma_k^\top \tilde{q}^{ss} \equiv 0. \tag{17}$$
It follows from $f(\xi_k) > 0$ that $\sigma_k^\top \tilde{q}^{ss} \equiv 0$. By Assumption III.2, $\tilde{q}^{ss}$ can be expressed as a linear combination of $\{\sigma_m\}_{m=1}^{\tau_0 - 1}$, i.e., $\tilde{q}^{ss} = \sum_{m=0}^{\tau_0-1} c_m^\ddagger \sigma_m$ for some constants $c_m^\ddagger \in \mathbb{R}$, then one has $\|\tilde{q}^{ss}\|^2 = \tilde{q}^{ss\top} \sum_{m=0}^{\tau_0-1} c_m^\ddagger \sigma_m = 0$, another contradiction.
2) $\phi_k \equiv 0$. In this case, one has $u_k = -\beta \hat{q}_k + Cf(\xi_k)\sigma_k = 0$, $q_k \equiv q^{ss}$, $\hat{q}_k \equiv \hat{q}^{ss}$ and $\xi_k \equiv \xi^{ss}$. On the other hand,
$$\begin{aligned} u_k &= -\beta \hat{q}^{ss} + Cf(\xi^{ss})\sigma_k = 0, \\ u_{k+\tau_0} &= -\beta \hat{q}^{ss} + Cf(\xi^{ss})\sigma_{k+\tau_0} = 0, \end{aligned} \tag{18}$$
which hold only if $\hat{q}^{ss} = 0$ and $\xi^{ss} = 0$. It follows from Assumption III.4 and Lemma III.7 that $p^{ss} = p^* + x^*$, i.e., $q^{ss} = 0$.
3) $\tilde{q}^{ss} = 0$. One has
$$q_{k+1} = q_k + Ts_k(-\beta q_k + Cf(\xi_k)\sigma_k), \tag{19}$$
then $\Delta M_k \le -Ts_k(\beta - C)\|q_k\|$, which implies that q_k converges to 0 for each trajectory.

This completes the proof. ∎

Remark III.12. *It can be seen that the parameter settings in Propositions III.9 and III.10 are the same with that in [15] while the key differences lie in analysis, i.e., the use of reverse triangle inequalities* (31) *and the proof of the global stability of* $q^{ss} = 0$ *with the sophisticated design of* ξ_k.

IV. Integrated Localization and Formation Control

In this section, we aim to generalize the distance-based relative docking to multi-robot formation control, where an integrated localization and formation control scheme is proposed to tackle Problem II.2. If each robot can measure the distance w.r.t. the landmark, then the formation control

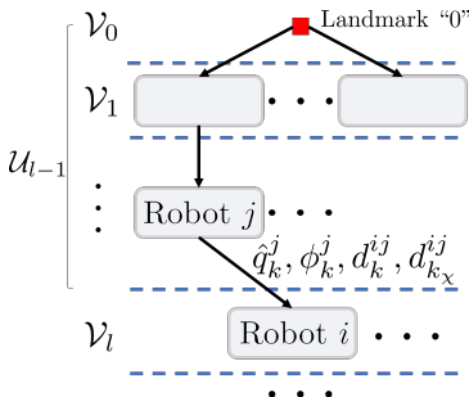

Fig. 3: An illustration of the control scheme for cooperative formation control. Each rounded rectangular represents a robot whose internal control diagram is the same with Fig. 1. The arrow from j to i denotes information transmissions through communication and local distance measurements w.r.t. robot j, $j \in \overline{\mathcal{N}}_i \subset \mathcal{U}_{l-1}$.

problem can be solved via applying (8) and (10) to each robot. However, it puts a heavy burden of communication on the landmark, and compromises the robustness in the case of link failure. Therefore, we would leverage on the cooperation among agents and design a distributed cooperative estimator and a motion controller for each agent which can communicate with and measure its distance to neighbors, but not necessarily to the landmark. In communication, we assume that each agent can transmit its own displacement measurements and their estimates of relative positions w.r.t. the landmark to its neighbors, see Fig. 3.

A. Cooperative adaptive estimator for localization

Denote the relative position to the desired docking position by $q_k^i = p_k^i - (p^* + x_i^*)$ and its estimate by $\hat{q}_k^i$. Denote $p_k^{ij} = p_k^i - p_k^j$ and $\hat{p}_k^{ij}$ its estimate. Let $q_k^{ij} = q_k^i - q_k^j$, $x_{ij}^* = x_i^* - x_j^*$ and $\phi_k^{ij} = \phi_k^i - \phi_k^j$, $p_k^0 = p^*$, $x_0^* = q_k^0 = 0$ and $\phi_k^0 = 0$. Observe that

$$\begin{aligned} d_{k+1}^{ij^2} - d_k^{ij^2} &= \|p_{k+1}^{ij}\|^2 - \|p_k^{ij}\|^2 \\ &= \|p_k^{ij} + \phi_k^{ij}\|^2 - \|p_k^{ij}\|^2 \\ &= \|\phi_k^{ij}\|^2 + 2\phi_k^{ij\top} p_k^{ij}, \end{aligned} \tag{20}$$

from which the following adaptive updating law can be designed:

$$\hat{p}_{k+1}^{ij} = \hat{p}_k^{ij} + \phi_k^{ij} + \Gamma \phi_k^{ij} \epsilon_{k+1}^{ij}, \ \forall (i,j) \in \overline{\mathcal{E}}, \tag{21}$$

where $\epsilon_{k+1}^{ij} = \frac{1}{2}(d_{k+1}^{ij^2} - d_k^{ij^2} - \|\phi_k^{ij}\|^2) - \phi_k^{ij\top} \hat{p}_k^{ij} = \phi_k^{ij\top} p_k^{ij} - \phi_k^{ij\top} \hat{p}_k^{ij}$. Then a consensus-based estimator for each $i \in \mathcal{V}$ can be designed as:

$$\hat{q}_{k+1}^i = \hat{q}_k^i + \phi_k^i + \sum_{j \in \overline{\mathcal{N}}_i} a_{ij} (\hat{p}_k^{ij} - (\hat{q}_k^i + x_i^* - \hat{q}_k^j - x_j^*)). \tag{22}$$

In the above, (21) is designed for estimating the relative position of neighbors, which are further fed into (22) to estimate the relative position to the landmark.

B. Cooperative motion controller

We assume that each agent i generates σ_k^i according to the autonomous system (9), which satisfies the following assumption.

Assumption IV.1. *For each $i \in \mathcal{V}$,*

1) *ρ_k^i is bounded, $\forall k \in \mathbb{Z}_{\geq 0}$, and $\sup_{k \in \mathbb{Z}_{\geq 0}} \|\sigma_k^i\| \leq 1$; and*
2) *there exists some constant $\tau_i \in \mathbb{Z}_+$ such that $\sigma_{k+\tau_i}^i = -\sigma_k^i$, $\forall k \in \mathbb{Z}_{\geq 0}$ and $\mathrm{Span}\{\sigma_0^i, \cdots, \sigma_{\tau_i - 1}^i\} = \mathbb{R}^n$.*

For robot i, the bounded input is designed as:

$$\overline{u}_k^i = \mathrm{proj}_U \, u_k^i, u_k^i = -\beta \hat{q}_k^i + Cf(\xi_k^i)\sigma_k^i, \tag{23}$$

where

$$\begin{aligned} \xi_k^i &= \max_{j \in \overline{\mathcal{N}}_i} \xi_k^{ij}, \\ \xi_k^{ij} &= \max(\zeta_k^{ij}, |d_k^{ij} - \|x_{ij}^*\||), \\ \zeta_k^{ij} &= \max_{\chi \in \{1, \cdots, \overline{n}_{ij}\}} (|\|x_{ij}^* - \sum_{t=k_\chi}^{k} \phi_t^{ij}\| - d_{k_\chi}^{ij}|), \overline{n}_{ij} \geq 0. \end{aligned} \tag{24}$$

In the above, we denote $\overline{n}_{ij}$ as the number of triggering instants of agent i for agent j, and we require the following assumption:

Assumption IV.2. *For each $i \in \mathcal{V}$, the coordinates of $\{x_j^* : j \in \overline{\mathcal{N}}_i\} \cup (\cup_{j \in \overline{\mathcal{N}}_i} \{p_{k_\chi}^{ij}\}_{\chi=1}^{\overline{n}_{ij}})$ satisfy*

$$\mathrm{Rank}([x_{jm}^*, \cdots, (p_{k_\chi}^{ij} + x_{im}^*), \cdots]) = n,$$

where $j, m \in \overline{\mathcal{N}}_i, \chi = 1, \cdots, \overline{n}_{ij}$.

Remark IV.3. *Note that the above assumption is different from Assumption III.4 as now we may rely on more than one neighbor to fulfill the relative localization. If agent i has less than $n+1$ neighbors, it requires some artificial constraints generated from ζ_k^{ij} in (24) such that Assumption IV.2 can be satisfied. Otherwise, if agent i has no less than $n+1$ neighbors and their desired formation is generic, then no other artificial constraints are needed.*

Remark IV.4. *Our method can be interpreted as spatio-temporal cooperative formation control, i.e., in addition to the spatial cooperation of inter-node distance measurements, we further exploit the temporal cooperation of intra-node displacement measurements. This setting shares some similarity with [24], where each agent performs a circular motion with different periods. However, [24] requires the signals to be commensurate for Fast Fourier Transform, which is a stronger requirement than Assumption III.2. Moreover, global stability and applicability in high dimensional spaces can be established by using our method with a weaker graphical condition, i.e., DAG.*

Remark IV.5. *Collision avoidance is not explicitly considered in our controller design. However, in practical implementation, it can be incorporated in the low-level motion controller by using techniques such as that in [36].*

C. Stability Analysis

In this subsection, we aim to analyze the stability of the integrated localization and formation control system. We prove the boundedness of signals under proper parameter settings and establish the convergence result by virtue of Lasalle's invariance principle.

Proposition IV.6. *Under the adaptive estimator* (21)*,* $\tilde{p}_k^{ij} \coloneqq \hat{p}_k^{ij} - p_k^{ij} \in \ell_\infty$ *if*

$$\gamma(2TU)^2 < 2. \tag{25}$$

Proof. See Appendix C. ∎

Proposition IV.7. *Under Assumption II.3 and the adaptive estimator* (21) *and* (22)*,* $\tilde{q}_k^i \coloneqq \hat{q}_k^i - q_k^i \in \ell_\infty$ *if condition* (25) *is satisfied.*

Proof. See Appendix D. ∎

Proposition IV.8. *Under Assumption II.3 and the motion controller* (23)*, there exists a constant* M_i *such that* $\limsup_{k\to\infty} \|q_k^i\| \leq M_i, i \in \mathcal{V}$*, if the conditions in Proposition IV.7 and* (15) *hold.*

Proof. See Appendix E. ∎

Consider agent $i \in \mathcal{V}_l$, whose dynamics can be rewritten as:

$$\begin{aligned} q_{k+1}^i &= q_k^i + T\phi_k^i, \\ \tilde{q}_{k+1}^i &= \tilde{q}_k^i - \sum_{j\in\overline{\mathcal{N}}_i} a_{ij}(\tilde{q}_k^i - \tilde{q}_k^j) + \upsilon_i, \\ \tilde{p}_{k+1}^{ij} &= (I - \Gamma\phi_k^{ij}\phi_k^{ij\top})\tilde{p}_k^{ij}, \\ \rho_{k+1}^i &= \Pi(\rho_k^i), \end{aligned} \tag{26}$$

where $j \in \overline{\mathcal{N}}_i \subset \mathcal{U}_{l-1}$. When all neighbors j are located at the desired position $p^* + x_j^*$, we have $\phi_k^j = 0$ and $\phi_k^{ij} = \phi_k^i$. Hence, we consider (26) as a cascade system with $\sum_{j\in\overline{\mathcal{N}}_i} a_{ij}\tilde{q}_k^j$ being an input to the following unforced system

$$\begin{aligned} q_{k+1}^i &= q_k^i + T\phi_k^i, \\ \tilde{q}_{k+1}^i &= \tilde{q}_k^i - \sum_{j\in\overline{\mathcal{N}}_i} a_{ij}(\tilde{q}_k^i - \tilde{p}_k^{ij}), \\ \tilde{p}_{k+1}^{ij} &= (I - \Gamma\phi_k^i\phi_k^{i\top})\tilde{p}_k^{ij}, \\ \rho_{k+1}^i &= \Pi(\rho_k^i). \end{aligned} \tag{27}$$

The following results are presented to characterize the state trajectory of (27).

Proposition IV.9. *Let* $q_j^{ss} = 0$*,* $\tilde{q}_j^{ss} = 0$*,* $\sum_{w\in\overline{\mathcal{N}}_j} \tilde{p}_{jw}^{ss} = 0$ *hold for all* $j \in \overline{\mathcal{N}}_i$*. Under Assumptions II.3, III.1, IV.1 and IV.2,* q_k^i*,* $\tilde{q}_k^i$ *and* $\sum_{j\in\overline{\mathcal{N}}_i} a_{ij}\tilde{p}_k^{ij}$ *converge to* 0 *for each trajectory of the unforced system* (27) *if gains are chosen to satisfy* (25) *and* (15)*.*

Proof. See Appendix F. ∎

Now, we are ready to present the following result.

Theorem IV.10. *Under Assumptions II.3, III.1, IV.1 and IV.2, Problem II.2 can be solved by adopting cooperative adaptive estimators* (21) *and* (22)*, and motion controller* (23) *with gains being chosen to satisfy* (25) *and* (15)*.*

Proof. We prove this by considering agent $i \in \mathcal{V}_l$ where l is taken from 1 to L. For $i \in \mathcal{V}_1$, it can be found that q_k^i, $\tilde{q}_k^i$ and $\sum_{j\in\overline{\mathcal{N}}_i} a_{ij}\tilde{p}_k^{ij}$ converge to 0 for each trajectory of the system by Theorem III.11. Then considering $i \in \mathcal{V}_2$, one has q_k^i, $\tilde{q}_k^i$ and $\sum_{j\in\overline{\mathcal{N}}_i} a_{ij}\tilde{p}_k^{ij}$ converge to 0 for each trajectory of unforced system (27) in view of Proposition IV.9. By Propositions IV.6, IV.7 and IV.8, one gets that every orbit of system (26) is bounded in the future. Then it follows from Theorem 1.1 in [37] that $q_i^{ss} = 0$, $i \in \mathcal{U}_2$, is globally asymptotically stable. Traversing all the nodes until $l = L$, one has $q_i^{ss} = 0$, $\forall i \in \mathcal{V}$ and this completes the proof. ∎

V. Simulation Examples

In this section, we will present two sets of simulation examples: one set for relative docking of a single robot in 2-D and 3-D spaces, respectively; and the other set for formation control of $N = 3$ robots in 2-D and 3-D spaces, respectively. The parameters for relative docking are set as follows: $U = 0.75m/s$, $T = 0.1s$, $\gamma = 10$, $a = 36$, $\beta = 2$, $C = 1$, $\hat{q}_0 = 0$, $\rho_0 = [1\ 0]^\top$, $b_1 = b_2 = 1$. p^* and x^* are set as $[5\ 5]^\top$ (resp. $[5\ 5\ 5]^\top$) and $[5\sqrt{3}\ \ -5]^\top$ (resp. $\sqrt{2}[5\sqrt{3}\ \ -5\ 10]^\top/2$) for 2-D (resp. 3-D). Π and Σ are chosen according to Remark III.3. For formation control simulations, let $x^* = [x_1^{*\top}, x_2^{*\top}, x_3^{*\top}]^\top = 10[0\ 1\ -1\ 0\ 1\ 0]^\top$ $(10[1\ 1\ 0\ 0\ 1\ 1\ 1\ 0\ 1]^\top$ for 3-D, which describes a regular tetrahedron), $a = [a_1, a_2, a_3]^\top = [24\ 36\ 24]^\top$,

$$A = \frac{1}{4}\begin{bmatrix} 0 & 0 & 0 \\ 0 & 0 & 0 \\ 1 & 1 & 0 \end{bmatrix}, \tag{28}$$

$a_{10} = a_{20} = 1/4$ and other parameters remain the same as in the relative docking tasks. The trajectories of a single robot (denoted by green solid lines) with 2-D and 3-D relative docking tasks are recorded in Figs. 4 and 6, respectively. Figs. 7 and 8 show the trajectories of robots with 2-D and 3-D formation control tasks, respectively. It can be found that all of the robots (red asterisks) converge to their desired positions (red circles) asymptotically. Fig. 5 shows the states of the robot with 2-D relative docking task.

In addition, additive white Gaussian noises with zero mean and variance of 10^{-4} have been added to both distance and odometry measurements. The trajectories of robots are denoted by light blue dash-dot lines as shown in Figs. 4, 6, 7 and 8. It can be found that the robots (denoted by red pentagrams) converge to a small neighborhood of the desired positions.

VI. Conclusion

In this paper, we have addressed the distance-based relative docking problem for a single robot and the distance-based spatio-temporal cooperative formation control problem for multiple robots. The former has been tackled by introducing multiple constraints constructed from measurements at several proper triggering time instants along motion trajectory. Furthermore, this idea has been extended to handle the latter problem such that the desired formation control can be achieved for directed acyclic graphs without using relative position measurements as the temporal cooperation has been

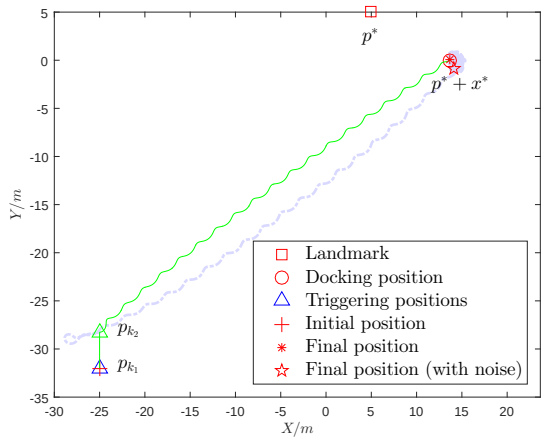

Fig. 4: The trajectory of robot with 2-D relative docking task. Trajectories under noise-free and noisy cases are denoted by green solid and light blue dash-dot lines, respectively. Figs. 6, 7 and 8 use the same legends.

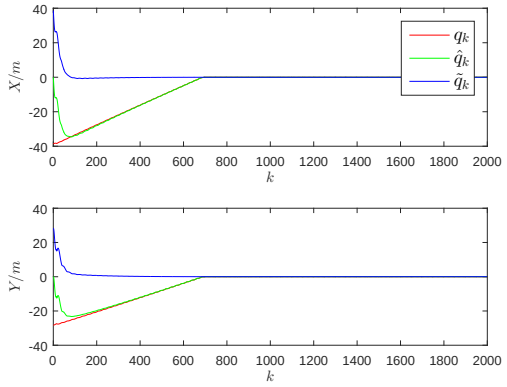

Fig. 5: States of robot with 2-D relative docking task (noise-free case).

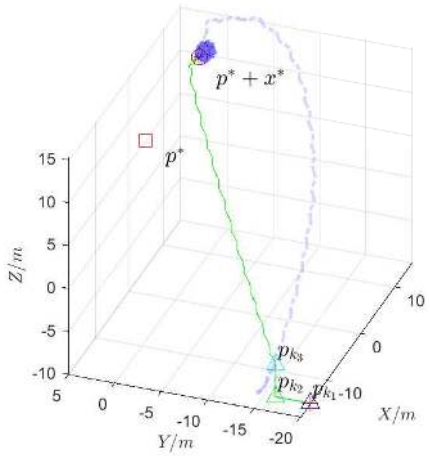

Fig. 6: The trajectory of robot with 3-D relative docking task.

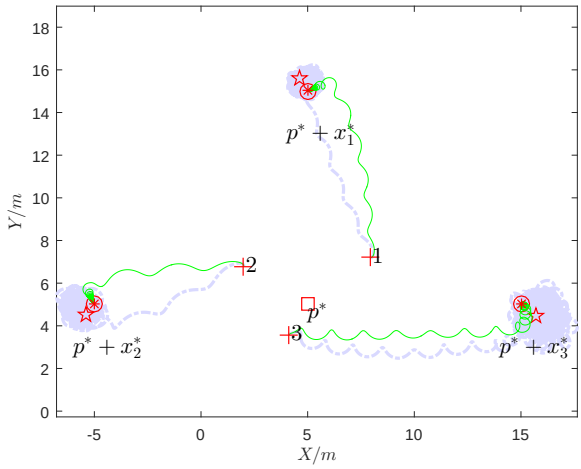

Fig. 7: Trajectories of robots with 2-D formation control task.

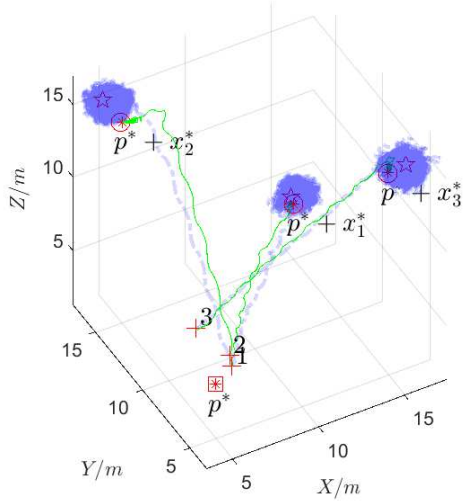

Fig. 8: Trajectories of robots with 3-D formation control task.

exploited. For both cases, the results of global asymptotical convergence have been rigorously established via discrete-time Lasalle's invariance principle.

Future work can be on the experimental validation and generalization to more general graphs (e.g. with cycles).

APPENDIX

A. *Proof of Proposition III.9*

It follows from (6), (8) and $\epsilon_{k+1} = -\phi_k^\top \tilde{q}_k$ that

$$\tilde{q}_{k+1} = \tilde{q}_k + \Gamma\phi_k\epsilon_{k+1} = (I - \Gamma\phi_k\phi_k^\top)\tilde{q}_k. \tag{29}$$

Let $V_k = \tilde{q}_k^\top\Gamma^{-1}\tilde{q}_k$ and $\Delta V_k = V_{k+1} - V_k$, one has

$$\Delta V_k = -\epsilon_{k+1}^2(2 - \phi_k^\top\Gamma\phi_k). \tag{30}$$

If $\gamma(TU)^2 < 2$, $\phi_k^\top\Gamma\phi_k = \gamma\|\phi_k\|^2 \leq \gamma(TU)^2 < 2$, or equivalently, $\Delta V_k \leq 0$. Thus, one has $V_k \leq V_{k-1} \leq \cdots \leq V_0$, i.e., $\tilde{q}_k$ is bounded. On the other hand, it follows from

the boundedness of ϕ_k that ϵ_{k+1} is also bounded. $\epsilon_{k+1} \in \ell_2$ follows from $\sum_{k=0}^{\infty} \Delta V_k = -\sum_{k=0}^{\infty} \epsilon_{k+1}^2(2-\gamma\|\phi_k\|^2) = \lim_{k\to\infty} V_{k+1} - V_0 \leq 0$.

B. Proof of Proposition III.10

Let $M_k = \|q_k\|$ and $\Delta M_k = M_{k+1} - M_k$. One has

$$\begin{aligned}\Delta M_k &= \|q_k + Ts_k(-\beta q_k - \beta\tilde{q}_k + Cf(\xi_k)\sigma_k)\| - \|q_k\| \\ &\leq |1-\beta Ts_k|\|q_k\| + \beta Ts_k\|\tilde{q}_k\| \\ &\quad + CTs_k|f(\xi_k)|\|\sigma_k\| - \|q_k\| \\ &\leq |1-\beta Ts_k|\|q_k\| + \beta Ts_k\|\tilde{q}_k\| \\ &\quad + CTs_k\|q_k\| - \|q_k\|,\end{aligned}$$

where we used the triangular inequality in the second line, while the last inequality follows from Assumption III.2, $s_k \in (0,1]$ and $f(\xi_k) \leq \xi_k \leq \|q_k\|$ in view of Assumption III.1 and the following reverse triangle inequalities

$$\begin{aligned}|d_k - \|x^*\|| &= |\|p_k - p^*\| - \|x^*\|| \\ &\leq \|(p_k - p^*) - x^*\| \\ &= \|q_k\|,\end{aligned}$$

$$\begin{aligned}|\|x^* - \sum_{l=k_\chi}^{k}\phi_l\| - d_{k_\chi}| &= |\|x^* - (p_k - p_{k_\chi})\| - \|p_{k_\chi} - p^*\|| \\ &\leq \|(x^* - (p_k - p_{k_\chi})) - (p_{k_\chi} - p^*)\| \\ &= \|q_k\|.\end{aligned} \tag{31}$$

Moreover, $\beta T < 1$ implies that

$$\begin{aligned}\Delta M_k &\leq (1 - \beta Ts_k + CTs_k - 1)\|q_k\| + \beta Ts_k\|\tilde{q}_k\| \\ &= Ts_k(C-\beta)\|q_k\| + \beta Ts_k\|\tilde{q}_k\|\end{aligned}$$

Therefore, it follows from $\beta > C$ that there exists some constant M' such that $\Delta M_k < 0$ if $\|q_k\| \geq M'$ as $\|\tilde{q}_k\|$ is bounded from Proposition III.9. Then one has $\Delta M_k < 0$, which completes the proof.

C. Proof of Proposition IV.6

It follows from (21) and $\epsilon_{k+1}^{ij} = -\phi_k^{ij\top}\tilde{p}_k^{ij}$ that

$$\tilde{p}_{k+1}^{ij} = (I - \Gamma\phi_k^{ij}\phi_k^{ij\top})\tilde{p}_k^{ij}. \tag{32}$$

Letting $V_k^{ij} = \tilde{p}_k^{ij\top}\Gamma^{-1}\tilde{p}_k^{ij}$ and $\Delta V_k^{ij} = V_{k+1}^{ij} - V_k^{ij}$, one has

$$\Delta V_k^{ij} = -\epsilon_{k+1}^{ij^2}(2 - \phi_k^{ij\top}\Gamma\phi_k^{ij}). \tag{33}$$

The rest of the proof follows that of Proposition III.9 and $\|\phi_k^{ij}\| \leq 2TU$ ($\|\phi_k^{i0}\| \leq TU \leq 2TU$).

D. Proof of Proposition IV.7

By (22), one has

$$\tilde{q}_{k+1}^i = \tilde{q}_k^i - \sum_{j\in\overline{\mathcal{N}}_i} a_{ij}(\tilde{q}_k^i - \tilde{q}_k^j) + \upsilon_i, i \in \mathcal{V}, \tag{34}$$

where $\upsilon_i = \sum_{j\in\overline{\mathcal{N}}_i} a_{ij}\tilde{p}_k^{ij}$.

Concatenating them together, one has

$$\tilde{q}_{k+1} = ((I_N - \mathcal{L}_0)\otimes I_n)\tilde{q}_k + \Upsilon, \tag{35}$$

where $\Upsilon = [\upsilon_1^\top, \cdots, \upsilon_N^\top]^\top$. By the proof of Theorem 4.2 in [33], Assumption II.3 and (5) imply that $(I_N - \mathcal{L}_0)$ is a Schur matrix and hence $\tilde{q}_k$ is bounded.

E. Proof of Proposition IV.8

We prove this by considering agent $i \in \mathcal{V}_l$, where l is taken from 1 to L.

Consider agent $i \in \mathcal{V}_1$, which only has the single neighbor from $\mathcal{V}_0$ (landmark 0). It follows from Proposition III.10 that $\limsup_{k\to\infty}\|q_k^i\| \leq M_i$, $\forall i \in \mathcal{V}_1$.

Next, consider agent $i \in \mathcal{V}_2$, which only has neighbors from previous layers $\mathcal{U}_1$. Let $M_k^i = \|q_k^i\|$ and $\Delta M_k^i = M_{k+1}^i - M_k^i$. By (23), one has

$$\begin{aligned}\Delta M_k^i &= \|q_k^i + Ts_k^i(-\beta q_k^i - \beta\tilde{q}_k^i + Cf(\xi_k^i)\sigma_k^i)\| - \|q_k^i\| \\ &\leq |1-\beta Ts_k^i|\|q_k^i\| + \beta Ts_k^i\|\tilde{q}_k^i\| \\ &\quad + CTs_k^i|f(\xi_k^i)|\|\sigma_k^i\| - \|q_k^i\| \\ &\leq |1-\beta Ts_k^i|\|q_k^i\| + \beta Ts_k^i\|\tilde{q}_k^i\| \\ &\quad + CTs_k^i\|q_k^i\| + \max_{j\in\overline{\mathcal{N}}_i} CTs_k^i\|q_k^j\| - \|q_k^i\|,\end{aligned} \tag{36}$$

where the last inequality results from the following reverse triangle inequalities

$$\begin{aligned}|d_k^{ij} - \|x_{ij}^*\|| &= |\|p_k^{ij}\| - \|x_{ij}^*\|| \\ &\leq \|(q_k^{ij} + x_{ij}^*) - x_{ij}^*\| \\ &= \|q_k^{ij}\| \leq \|q_k^i\| + \|q_k^j\|,\end{aligned}$$

$$\begin{aligned}|\|x_{ij}^* - \sum_{t=k_\chi}^{k}\phi_t^{ij}\| - d_{k_\chi}^{ij}| &= |\|x_{ij}^* - (p_k^{ij} - p_{k_\chi}^{ij})\| - \|p_{k_\chi}^{ij}\|| \\ &\leq \|x_{ij}^* - (p_k^{ij} - p_{k_\chi}^{ij}) - p_{k_\chi}^{ij}\| \\ &= \|q_k^{ij}\| \leq \|q_k^i\| + \|q_k^j\|.\end{aligned} \tag{37}$$

Since $j \in \overline{\mathcal{N}}_i \subset \mathcal{U}_1$ by Assumption II.3 and the boundedness of $\|q_k^j\|$ is proved above, we can prove that $\limsup_{k\to\infty}\|q_k^i\| \leq M_i$, $\forall i \in \mathcal{V}_2$ by following the proof of Proposition III.10.

Traversing all the nodes until $l = L$, one has $\limsup_{k\to\infty}\|q_k^i\| \leq M_i$, $\forall i \in \mathcal{V}$, which completes the proof.

F. Proof of Proposition IV.9

By the boundedness result of Propositions IV.7, IV.6 and IV.8, as well as Assumption III.2, we can invoke Lasalle's invariance principle [28] to show all trajectories will converge to the largest invariant set $\mathcal{M}_i$ included in $\{[q_k^{i\top}, \tilde{q}_k^{i\top}, \tilde{p}_k^{ij\top}, \rho_k^{i\top}]^\top \in \mathbb{R}^{(3+\mathrm{Card}(\overline{\mathcal{N}}_i))n} \mid \Delta V_k^i = \sum_{j\in\overline{\mathcal{N}}_i}\Delta V_k^{ij} = 0\}$, where V^{ij} is the Lyapunov function defined in the proof of Proposition IV.6. It suffices to show that $q_k^i \equiv 0$ holds for any trajectory $\{[q_k^{i\top}, \tilde{q}_k^{i\top}, \tilde{p}_k^{ij}, \rho_k^{i\top}]^\top\}_{k\in\mathbb{Z}_{\geq 0}}$ in $\mathcal{M}_i$.

It follows from (33) that $\Delta V_k^i \equiv 0$ iff $\epsilon_{k+1}^{ij} = -\phi_k^{i\top}\tilde{p}_k^{ij} \equiv 0$, $\forall j \in \overline{\mathcal{N}}_i$, which also follows from (32) and the second equation of (27) that $\tilde{p}_k^{ij} \equiv \tilde{p}_{ij}^{ss}$ and $\tilde{q}_k^i \equiv \tilde{q}_i^{ss} = \sum_{j\in\overline{\mathcal{N}}_i} a_{ij}\tilde{p}_{ij}^{ss} / \sum_{j\in\overline{\mathcal{N}}_i} a_{ij}$. It suffices to show that $\phi_k^{i\top}\tilde{p}_{ij}^{ss} \equiv 0$, $\forall j \in \overline{\mathcal{N}}_i$, is equivalent to $q_i^{ss} = 0$. Similar to the proof of Theorem III.11, we consider the following three cases: 1) $\phi_k^i \not\equiv 0$ and $\exists r \in \overline{\mathcal{N}}_i$, $\tilde{p}_{ir}^{ss} \neq 0$; 2) $\phi_k^i \equiv 0$; and 3) $\forall j \in \overline{\mathcal{N}}_i$, $\tilde{p}_{ij}^{ss} = 0$.

For Case 1), since

$$0 \equiv \phi_k^{i\top}\tilde{p}_k^{ij} = (q_{k+1}^i - q_k^i)^\top\tilde{p}_{ij}^{ss} = (\hat{q}_{k+1}^i - \hat{q}_k^i)^\top\tilde{p}_{ij}^{ss} \tag{38}$$

for all $j \in \overline{\mathcal{N}}_i$, one has $\hat{q}_k^{i\top}\tilde{p}_{ij}^{ss} \equiv c_{ij}^{\dagger}$ for some constant $c_{ij}^{\dagger} \in \mathbb{R}$. On the other hand, $0 \equiv \phi_k^{i\top}\tilde{p}_{ij}^{ss}$ also implies that $0 \equiv \phi_k^{i\top}\tilde{p}_{ij}^{ss} = [-\beta\hat{q}_k^i + Cf(\xi_k^i)\sigma_k^i]^{\top}\tilde{p}_{ij}^{ss}$, or equivalently $\beta c_{ij}^{\dagger} \equiv \beta\hat{q}_k^{i\top}\tilde{p}_{ij}^{ss} = Cf(\xi_k^i)\sigma_k^{i\top}\tilde{p}_{ij}^{ss}$. Specifically, we have $f(\xi_k^i)\sigma_k^{i\top}\tilde{p}_{ij}^{ss} = f(\xi_{k+\tau_{ij}}^i)\sigma_{k+\tau_{ij}}^{i\top}\tilde{p}_{ij}^{ss}$, $\forall j \in \overline{\mathcal{N}}_i$, where τ_{ij} is the least common multiple of τ_i and τ_j. Next we establish $f(\xi_k^i) > 0$ by contradiction. Suppose $f(\xi_k^i) = 0$, one has $p_k^i = p^* + x_i^*$ by Assumption III.4, Lemma III.7 and the fact that agent j is located at the desired position $p^* + x_j^*$, $\forall j \in \overline{\mathcal{N}}_i \subset \mathcal{U}_l$. Then it follows from $u_k^i = -\beta\hat{q}_k^i = -\beta\tilde{q}_i^{ss} = -\beta\sum_{j\in\overline{\mathcal{N}}_i} a_{ij}\tilde{p}_{ij}^{ss} / \sum_{j\in\overline{\mathcal{N}}_i} a_{ij}$ that u_k^i is a linear combination of $\tilde{p}_{ij}^{ss}$, $j \in \overline{\mathcal{N}}_i$. By (38), one has $\phi_k^{i\top}\tilde{p}_{ij}^{ss} = Ts_k^i u_k^{i\top}\tilde{p}_{ij}^{ss} = 0$, which implies that u_k^i is orthogonal to $\tilde{p}_{ij}^{ss}$ for all $j \in \overline{\mathcal{N}}_i$, a contradiction. Therefore, $f(\xi_k^i) > 0$, $\forall k \in \mathbb{Z}_{\geq 0}$.

On the other hand, by $\sigma_{k+\tau_{ir}}^i = -\sigma_k^i$, we have

$$[f(\xi_k^i) + f(\xi_{k+\tau_{ir}}^i)]\sigma_k^{i\top}\tilde{p}_{ir}^{ss} \equiv 0. \tag{39}$$

It follows from $f(\xi_k^i) > 0$ that $\sigma_k^{i\top}\tilde{p}_{ir}^{ss} \equiv 0$. By Assumption III.2, one has $\tilde{p}_{ir}^{ss} = \sum_{m=0}^{\tau_i-1} c_{ij,m}^{\ddagger}\sigma_m^i$ for some $c_{ij,m}^{\ddagger} \in \mathbb{R}$ and hence $\|\tilde{p}_{ir}^{ss}\|^2 = \tilde{p}_{ir}^{ss\top}\sum_{m=0}^{\tau_i-1} c_{ij,m}^{\ddagger}\sigma_m^i = 0$, another contradiction.

It can be easily obtained from Case 2) and 3) that q_k^i, $\tilde{q}_k^i$ and $\sum_{j\in\overline{\mathcal{N}}_i} a_{ij}\tilde{p}_k^{ij}$ converge to 0 for each trajectory by following the proof of Theorem III.11.

REFERENCES

[1] J. Hu, J. Xu, and L. Xie, "Cooperative search and exploration in robotic networks," *Unmanned Systems*, vol. 1, no. 1, pp. 121–142, 2013.

[2] P. Ogren, E. Fiorelli, and N. E. Leonard, "Cooperative control of mobile sensor networks: Adaptive gradient climbing in a distributed environment," *IEEE Transactions on Automatic Control*, vol. 49, no. 8, pp. 1292–1302, 2004.

[3] R. W. Beard, T. W. McLain, D. B. Nelson, D. Kingston, and D. Johanson, "Decentralized cooperative aerial surveillance using fixed-wing miniature uavs," *Proceedings of the IEEE*, vol. 94, no. 7, pp. 1306–1324, 2006.

[4] Y. Yue, C. Yang, Y. Wang, P. C. N. Senarathne, J. Zhang, M. Wen, and D. Wang, "A multilevel fusion system for multirobot 3-d mapping using heterogeneous sensors," *IEEE Systems Journal*, published online, 2019.

[5] D. Fox, W. Burgard, H. Kruppa, and S. Thrun, "A probabilistic approach to collaborative multi-robot localization," *Autonomous robots*, vol. 8, no. 3, pp. 325–344, 2000.

[6] Z. Xiao, Y. Hei, Q. Yu, and K. Yi, "A survey on impulse-radio uwb localization," *Science China Information Sciences*, vol. 53, no. 7, pp. 1322–1335, 2010.

[7] Z. Yan, N. Jouandeau, and A. A. Cherif, "A survey and analysis of multi-robot coordination," *International Journal of Advanced Robotic Systems*, vol. 10, no. 12, p. 399, 2013.

[8] G. Cai, J. Dias, and L. Seneviratne, "A survey of small-scale unmanned aerial vehicles: Recent advances and future development trends," *Unmanned Systems*, vol. 2, no. 02, pp. 175–199, 2014.

[9] S. Zhao and D. Zelazo, "Localizability and distributed protocols for bearing-based network localization in arbitrary dimensions," *Automatica*, vol. 69, pp. 334–341, 2016.

[10] Z. Lin, T. Han, R. Zheng, and M. Fu, "Distributed localization for 2-d sensor networks with bearing-only measurements under switching topologies." *IEEE Transactions on Signal Processing*, vol. 64, no. 23, pp. 6345–6359, 2016.

[11] A. Chakraborty, S. Misra, R. Sharma, and C. N. Taylor, "Observability conditions for switching sensing topology for cooperative localization," *Unmanned Systems*, vol. 5, no. 03, pp. 141–157, 2017.

[12] M. Z. Win, Y. Shen, and W. Dai, "A theoretical foundation of network localization and navigation," *Proceedings of the IEEE*, vol. 106, no. 7, pp. 1136–1165, 2018.

[13] B. Fidan, S. Dasgupta, and B. D. Anderson, "Adaptive range-measurement-based target pursuit," *International Journal of Adaptive Control and Signal Processing*, vol. 27, no. 1-2, pp. 66–81, 2013.

[14] S. Güler, B. Fidan, S. Dasgupta, B. D. Anderson, and I. Shames, "Adaptive source localization based station keeping of autonomous vehicles," *IEEE Transactions on Automatic Control*, vol. 62, no. 7, pp. 3122–3135, 2017.

[15] T.-M. Nguyen, Z. Qiu, M. Cao, T. H. Nguyen, and L. Xie, "Single landmark distance-based navigation," *IEEE Transactions on Control Systems Technology*, published online, 2019.

[16] W. Ren, R. W. Beard, and E. M. Atkins, "Information consensus in multivehicle cooperative control," *IEEE Control Systems Magazine*, vol. 27, no. 2, pp. 71–82, 2007.

[17] R. Olfati-Saber and R. M. Murray, "Consensus problems in networks of agents with switching topology and time-delays," *IEEE Transactions on Automatic Control*, vol. 49, no. 9, pp. 1520–1533, 2004.

[18] M. Ji and M. Egerstedt, "Distributed coordination control of multiagent systems while preserving connectedness," *IEEE Transactions on Robotics*, vol. 23, no. 4, pp. 693–703, 2007.

[19] L. Krick, M. E. Broucke, and B. A. Francis, "Stabilisation of infinitesimally rigid formations of multi-robot networks," *International Journal of Control*, vol. 82, no. 3, pp. 423–439, 2009.

[20] S. Zhao and D. Zelazo, "Bearing rigidity and almost global bearing-only formation stabilization," *IEEE Transactions on Automatic Control*, vol. 61, no. 5, pp. 1255–1268, 2016.

[21] G. Jing, G. Zhang, H. W. J. Lee, and L. Wang, "Angle-based shape determination theory of planar graphs with application to formation stabilization," *Automatica*, vol. 105, pp. 117–129, 2019.

[22] K. Cao, Z. Han, X. Li, and L. Xie, "Ratio-of-distance rigidity theory with application to similar formation control," *IEEE Transactions on Automatic Control*, published online, 2019.

[23] M. Cao, C. Yu, and B. D. Anderson, "Formation control using range-only measurements," *Automatica*, vol. 47, no. 4, pp. 776–781, 2011.

[24] B. Jiang, M. Deghat, and B. D. Anderson, "Simultaneous velocity and position estimation via distance-only measurements with application to multi-agent system control," *IEEE Transactions on Automatic Control*, vol. 62, no. 2, pp. 869–875, 2017.

[25] M. Ye, B. D. Anderson, and C. Yu, "Bearing-only measurement self-localization, velocity consensus and formation control," *IEEE Transactions on Aerospace and Electronic Systems*, vol. 53, no. 2, pp. 575–586, 2017.

[26] Z. Han, K. Guo, L. Xie, and Z. Lin, "Integrated relative localization and leader–follower formation control," *IEEE Transactions on Automatic Control*, vol. 64, no. 1, pp. 20–34, 2019.

[27] Y. Cai and Y. Shen, "Integrated localization and control for accurate multi-agent formation," in *2018 IEEE International Conference on Communications (ICC)*. IEEE, 2018, pp. 1–6.

[28] W. Mei and F. Bullo, "Lasalle invariance principle for discrete-time dynamical systems: A concise and self-contained tutorial," *arXiv preprint arXiv:1710.03710*, 2017.

[29] K. Cao, Z. Qiu, and L. Xie, "Relative docking via range-only measurements," in *2019 15th IEEE International Conference on Control & Automation (ICCA)*, to appear.

[30] H. G. Tanner, G. J. Pappas, and V. Kumar, "Leader-to-formation stability," *IEEE Transactions on Robotics and Automation*, vol. 20, no. 3, pp. 443–455, 2004.

[31] W. Ding, G. Yan, and Z. Lin, "Collective motions and formations under pursuit strategies on directed acyclic graphs," *Automatica*, vol. 46, no. 1, pp. 174–181, 2010.

[32] W. Wang, C. Wen, J. Huang, and Z. Li, "Hierarchical decomposition based consensus tracking for uncertain interconnected systems via distributed adaptive output feedback control," *IEEE Transactions on Automatic Control*, vol. 61, no. 7, pp. 1938–1945, 2015.

[33] G. Chai, C. Lin, Z. Lin, and W. Zhang, "Consensus-based cooperative source localization of multi-agent systems with sampled range measurements," *Unmanned Systems*, vol. 2, no. 3, pp. 231–241, 2014.

[34] Wikipedia contributors, "Unmanned vehicle — Wikipedia, the free encyclopedia," 2019, [Online; accessed 05-June-2019]. [Online]. Available: https://en.wikipedia.org/wiki/Unmanned_vehicle

[35] B. Fidan and I. Umay, "Adaptive environmental source localization and tracking with unknown permittivity and path loss coefficients," *Sensors*, vol. 15, no. 12, pp. 31 125–31 141, 2015.

[36] L. Wang, A. D. Ames, and M. Egerstedt, "Safety barrier certificates for collisions-free multirobot systems," *IEEE Transactions on Robotics*, vol. 33, no. 3, pp. 661–674, 2017.

[37] P. Seibert and R. Suarez, "Global stabilization of nonlinear cascade systems," *Systems & Control Letters*, vol. 14, no. 4, pp. 347–352, 1990.

Kun Cao received the B.Eng. degree in Mechanical engineering from the Tianjin University, Tianjin, China, in 2016. He is currently pursuing Ph.D. degree in the School of Electrical and Electronic Engineering, Nanyang Technological University, Singapore.

His research interests include formation control, distributed optimization, and soft robotics.

Zhirong Qiu received the B.Sc. and M.Sc. degrees in applied mathematics from Sun Yat-Sen University, Guangzhou, China in 2010 and 2012, respectively, and the Ph.D. degree in Electrical and Electronic Engineering from Nanyang Technological University, Singapore, in 2017. His research interests include multi-agent systems and distributed optimization.

Lihua Xie (F'07) received the B.E. and M.E. degrees in electrical engineering from Nanjing University of Science and Technology in 1983 and 1986, respectively, and the Ph.D. degree in electrical engineering from the University of Newcastle, Australia, in 1992. Since 1992, he has been with the School of Electrical and Electronic Engineering, Nanyang Technological University, Singapore, where he is currently a professor and Director, Delta-NTU Corporate Laboratory for Cyber-Physical Systems. He served as the Head of Division of Control and Instrumentation from July 2011 to June 2014. He held teaching appointments in the Department of Automatic Control, Nanjing University of Science and Technology from 1986 to 1989.

Dr Xie's research interests include robust control and estimation, networked control systems, multi-agent networks, localization and unmanned systems. He is an Editor-in-Chief for Unmanned Systems and an Associate Editor for IEEE Transactions on Network Control Systems. He has served as an editor of IET Book Series in Control and an Associate Editor of a number of journals including IEEE Transactions on Automatic Control, Automatica, IEEE Transactions on Control Systems Technology, and IEEE Transactions on Circuits and Systems-II. He was an elected member of Board of Governors, IEEE Control System Society (Jan 2016-Dec 2018). Dr Xie is a Fellow of IEEE and Fellow of IFAC.